Elsevier Editorial System(tm) for Industrial Crops and Products

Manuscript Draft

Manuscript Number: INDCRO-D-19-03145R2

Title: Production and characterization of lignin containing nanocellulose from luffa through an acidic deep eutectic solvent treatment and systematic fractionation

Article Type: Research Paper

Section/Category: Fibres, proteins and carbohydrates

Keywords: Acidic deep eutectic solvent, Cellulose nanofibers, Luffa sponge, Lignin containing nanocellulose

Corresponding Author: Dr. Hailan Lian, Ph.D.

Corresponding Author's Institution: Nanjing Forestry University

First Author: Shu Hong

Order of Authors: Shu Hong; Yandan Song; Yang Yuan; Hailan Lian, Ph.D.; Henrikki Liimatainen, Ph.D.

Abstract: In this study, lignin and hemicelluloses were partially separated from non-wood biomass of luffa sponge using an acidic deep eutectic solvent (ADES) composed of choline chloride and oxalic acid dihydrate, and the obtained cellulose-rich residue was further disintegrated into lignin containing cellulose nanocrystal (OA-CNC) and nanofiber (OA-CNF) fractions with a two-step ultrasonication treatment. The ADES had a dual purpose: to produce fractions of biomass and to accelerate the nanofibrillation of cellulose. Under optimal reaction conditions (at 90 °C for 150 min), solid fractions with cellulose content of 76.4 wt% (initially 51.8 wt%) and residual lignin content of 10.7 wt% (initially 17.8 wt%) were achieved. Ultrasonication resulted in lignin containing nanocelluloses with a high total yield (59.1 wt% vs. 50.5 wt% from reference 60% sulfuric acid hydrolysis). They consisted mainly of elongated cellulose nanofibers (OA-CNF) with an average diameter of 28 nm. The OA-CNF were further converted to flexible and foldable self-standing films with tensile strength of 134 MPa and elongation at break of 10.6%. This simplified method also presents great potential for using biomass waste (e.g., wheat straw, branches, and sawdust) to produce lignin containing nanocellulose.

Dear Editor in chief,

We are truly grateful to yours and other reviewers' critical comments and thoughtful suggestions on our manuscript (INDCRO-D-19-03145R1). Based on these comments and suggestions, we have made careful modifications on the manuscript. All changes made to the text are in red color. We hope the new manuscript will meet your journal's standard. We hope that these revisions are satisfactory and that the revised version will be acceptable for publication in Industrial Crops and Products. We appreciate for Editors/Reviewers' warm work earnestly and valuable comments on our work.

Thank you very much for your work concerning our paper.

Yours sincerely,

Hailan Lian

lianhailan@njfu.edu.cn

Detailed Response to Reviewers

Paper Title: Production and characterization of lignin containing nanocellulose from luffa through an acidic deep eutectic solvent treatment and systematic fractionation
Ms. No.: INDCRO-D-19-03145R1

Dear Editor-in-Chief,

We would like to thank you and all reviewers for the constructive feedback and great advices given in the comments. Below are all the comments with our answers. Responses to reviewers' comments are shown in blue. The revised parts were used red font in the manuscript accordingly.

Reviewer #1: Thanks for revising carefully.

This part of the response can go under "yield & characterisation of nanocellulose" section in Results and Discussion "After the DES treatment, the residue was washed and separated by centrifugation, i.e. turbid supernatant and solid residue. The followed ultrasonication treatment for these two parts led to CNC (turbid supernatant) and CNF (solid residue), respectively. Through the TEM results, the residual parts are all long fiber-like (> 500 nm in length). CNCs are rod-like or whisker-shaped nanoparticles with 3-5 nm in width and 50-500 nm in length. As CNFs are typically produced through mechanical refining, the nanoparticles have a higher aspect ratio with 4-20 nm in width and 500-2000 nm in length (Moon et al 2011, Chem Soc Rev). Therefore, we defined the residual parts as CNF. Moon R J, Martini A, Nairn J, et al. Cellulose nanomaterials review: structure, properties and nanocomposites[J]. Chemical Society Reviews, 2011, 40(7): 3941-3994."
Response: Thank you for your advice. We have added this part in the beginning of 'The yield and morphology of nanocelluloses' section.
Sincerely yours,
Hanlan Lian
Nanjing Forestry University, China

Highlights:

1. One step fraction and accelerating nanofibrillation of luffa sponge in deep eutectic solvent (DES).

2. Lignin containing nanocellulose fibers were liberated after ultrasonication treatment.

3. The self-standing nanopaper showed high mechanical strength.

Production and characterization of lignin containing nanocellulose from luffa through an acidic deep eutectic solvent treatment and systematic fractionation

*Shu Hong [a, b], Yandan Song [a], Yang Yuan [a], Hailan Lian [a, *], Henrikki Liimatainen [b]*

[a] College of Materials Science and Engineering, Nanjing Forestry University, Nanjing, 210037 China.

[b] Fibre and Particle Engineering Research Unit, University of Oulu, P.O. Box 4300, FI-90014, Finland.

Abstract: In this study, lignin and hemicelluloses were partially separated from non-wood biomass of luffa sponge using an acidic deep eutectic solvent (ADES) composed of choline chloride and oxalic acid dihydrate, and the obtained cellulose-rich residue was further disintegrated into lignin containing cellulose nanocrystal (OA-CNC) and nanofiber (OA-CNF) fractions with a two-step ultrasonication treatment. The ADES had a dual purpose: to produce fractions of biomass and to accelerate the nanofibrillation of cellulose. Under optimal reaction conditions (at 90 °C for 150 min), solid fractions with cellulose content of 76.4 wt% (initially 51.8 wt%) and residual lignin content of 10.7 wt% (initially 17.8 wt%) were achieved. Ultrasonication resulted in lignin containing nanocelluloses with a high total yield (59.1 wt% vs. 50.5 wt% from reference 60% sulfuric acid hydrolysis). They consisted mainly of elongated cellulose nanofibers (OA-CNF) with an average diameter of 28 nm. The OA-CNF were further converted to flexible and foldable self-standing films with tensile strength of 134 MPa and elongation at break of 10.6%. This simplified method also presents great potential for using biomass waste (e.g., wheat straw, branches, and sawdust) to produce lignin containing nanocellulose.

* *Corresponding author: Hailan Lian (lianhailan@njfu.edu.cn), Tel./fax: (86-25) 85427531.*

Keywords: Acidic deep eutectic solvent, Cellulose nanofibers, Luffa sponge, Lignin containing nanocellulose

1. Introduction

In the last few decades, bio-based nanomaterials derived from celluloses, i.e., cellulose nanocrystals (CNC) and nanofibers (CNF), have been under intensive research due to their many appealing characteristics, such as high strength, light weight, large specific surface area, biodegradability, and tailorable surface features (Nascimento and Rezende, 2018; Rosa et al., 2010). These green nanomaterials are typically prepared from pre-treated, delignified chemical pulp, which can be produced from various biomasses. The chemical pre-processing includes commonly harsh alkali cooking, bleaching, and other processes to remove lignin, hemicelluloses, and other compounds such as extractives and inorganics in order to obtain pulp with a high cellulose content. Strong acid or oxidation treatments combined with mechanical disintegration processes are further used to individualize CNC and CNF from chemically pre-treated biomass (Chen et al., 2015; Saito and Isogai, 2004). Consequently, several processing steps based on extensive use of toxic and harmful chemicals are typically required to produce nanocelluloses.

Recent studies (Bian et al., 2017b; Diop et al., 2017; Huang et al., 2019) have shown that cellulose nanomaterials can also be obtained from lignin containing raw materials. The use of unbleached pulp or pulp without extensive delignification could reduce the use of chemicals and energy consumption in nanocellulose production and provide lignin containing nanocelluloses (LCN) (Osong et al., 2013). In addition, residual lignin incorporated to nanocellulose has been reported to have several advantages, such as high thermal stability (Bian et al., 2017a; Nair and Yan, 2015), increased hydrophobicity (Poletto et al., 2012), UV-blocking properties (Sadeghifar et al., 2017), and antioxidant activity (Farooq et al., 2019). The LCN has shown also improved compatibility with hydrophobic polymer matrices as reinforcement in composites (Nair et al., 2018), and was found to significantly increase the mechanical,

thermal, and water barrier properties of the resulting composite (Nair et al., 2017). Therefore, the production of lignin containing nanocellulose directly from biomass may have significant practical applications.

Compared with delignified cellulose raw materials, biomass with a high concentration of lignin is difficult to disintegrate down to nanoscale due to the cross-linked barrier properties of lignin (Hoeger et al., 2013; Spence et al., 2010). Previously, p-toluenesulfonic acid solution has been used to dissolve and remove lignin from waste wheat straw, bark, and wood in order to improve cellulose nanofibrillation and further to produce lignin containing CNF using disk grinding (Bian et al., 2017b; Bian et al., 2019; Bian et al., 2018; Dou et al., 2019). Recently, it was also found that lignin can be solubilized in some acidic deep eutectic solvents (ADESs), such as choline chloride-lactic acid (ChCl-LA) and choline chloride-oxalic acid (ChCl-OA) (Alvarezvasco et al., 2016; Guo et al., 2019; Hong et al., 2016; Liu et al., 2017b; Lynam et al., 2017; Shen et al., 2019). Moreover, ADESs can be harnessed for efficient extraction and fractionation of biomasses to separate their main constituents (Alvarezvasco et al., 2016; Jablonsky et al., 2018; Liu et al., 2017b). ADESs such as ChCl-OA dihydrate can also act as hydrolytic media to depolymerize amorphous regions of cellulose and to liberate cellulose nanocrystals after mechanical disintegration (Sirviö et al., 2016). Since oxalic acid is a dicarboxylic acid, the unreacted free carboxyl group in cellulose can improve the dispersion of nanocellulose (Fan et al., 2008; Sirviö et al., 2016). The ChCl-OA DES was also used to develop a biorefinery approach based on lignin utilization, while simultaneously maintaining the cellulose available to produce nanocellulose (Liu et al., 2017b; Ma et al., 2019). The removal of lignin matrix from biomass and surface carboxylation of cellulose can in turn significantly reduce energy consumption of nanocellulose production and improve the homogeneity of nanocellulose (Lee et al., 2018; Meng et al., 2019). Moreover, oxalic acid can be obtained from natural sources and it is easy to recover (Lacerda et al., 2015). Therefore, ADESs show a promising and dual role in

processing of biomasses, i.e. they can be used both for fractionation of biomass and accelerate the nanofibrillation of cellulose.

Luffa is a tropical non-wood plant that belongs to the family of *Cucurbitaceae*. As a natural cellular material, it is typically used as a raw material for energy-absorption materials (Shen et al., 2012), as a template to fabricate porous materials (Alshaaer et al., 2017; Zampieri et al., 2006), and for water absorption or waste water treatment (Demir et al., 2006; Laidani et al., 2011), and is an appealing source for many other advanced applications due to its high cellulose content, which ranges from 55 to 90% (Siqueira et al., 2010). In addition to cellulose, luffa contains 10–23% lignin and 8–22% hemicelluloses (Chen et al., 2018). In this study, a deep eutectic solvent based on ChCl-OA dihydrate was used to partially delignify luffa biomass and separate a cellulose-rich solid fraction. Subsequently, the obtained residue underwent a two-step ultrasonication treatment to produce lignin containing cellulose nanofiber and nanocrystal fractions. Sulfuric acid hydrolysis of pristine and DES-treated luffa was used as a reference treatment. The physicochemical properties of nanocelluloses were determined using transmission electron microscopy (TEM), Fourier transform infrared spectroscopy (FTIR), elemental analysis, surface charge measurement, X-ray diffraction (XRD), and thermogravimetric analysis (TGA). The mechanical properties of lignin containing nanocelluloses were determined by tensile strength measurement from self-standing nanocellulose films.

2. Materials and methods

2.1. Materials

Luffa was collected from Xuchang City, Henan province, China. The water, extractive, and ash contents of the raw luffa were 9.03 wt%, 0.80 wt%, and 0.23 wt%, respectively. The luffa was first washed with tap water to remove water soluble impurities and dried in an oven at 100 °C for 6 h. The extractives were removed by sequential Soxhlet extractions with ethanol and ethanol/benzene (1:2, v/v) for 6 h. The cellulose, hemicellulose, and lignin contents in luffa were determined according to the

NREL's (National Renewable Energy Laboratory) standard procedure (Sluiter et al., 2010). The analysis was conducted in a high-performance liquid chromatography system (HPLC, Agilent 1200, Agilent, Germany) and an ultraviolet spectrophotometer (UV, Ultrospec 2100 Pro, Amersham, USA). The cellulose, hemicellulose, and lignin contents were 51.8 wt%, 17.5 wt%, and 17.8wt %, respectively.

Choline chloride and oxalic acid dihydrate were purchased from Sinopharm Chemical Reagent Co., Ltd. (Shanghai, China). Sulfuric acid (H_2SO_4, 98%), absolute ethyl alcohol, sodium hydroxide, and benzene were purchased from Nanjing Chemical Reagent Co., Ltd. All chemicals were of analytical grade and used without further purification.

2.2. Methods

Partial delignification of luffa in a DES

A DES of ChCl-OA dihydrate with a molar ratio of 1:1 was prepared by mixing the two components, choline chloride and oxalic acid dihydrate, in an oil bath at 100 °C until a transparent and homogeneous solution was formed. Luffa samples were fractionated in the DES with a mass ratio of 1:20 at the given temperatures (70, 80, 90, and 100 °C) for the desired times (1, 1.5, 2, and 2.5 h). The reaction was quenched by adding deionized (DI) water, and the mixture was then washed using a centrifuge (TDL-40B, Anting, China) at 4000 rpm for 5 min until the supernatant became colorless. The solid residue was used for detailed component analysis. The DES-soluble components of luffa in the supernatant were calculated by deducting the ones in the solid residue.

Preparation and fractionation of nanocellulose from DES-treated luffa via ultrasonication

The undried cellulose-rich residue from the DES treatment was diluted in water to 1 wt%, and was further washed several times with DI water and separated with a centrifuge (TDL-40B, Anting, China) at 4000 rpm for 5 min until the supernatant became turbid. The turbid supernatant suggested the presence of cellulose

nanocrystals (CNCs) (Bian et al., 2017a; Mao et al., 2017). The turbid supernatant was collected until the supernatant in the centrifugal tubes became transparent. The possible residues of the DES in the cellulose fraction were removed by dialysis in DI water using a dialysis tube with molecular weight cut-off (MWCO) of 12–14K (Viskase Companies, Darien, IL, USA) at room temperature for 7 days until the solution pH became neutral. Finally, the turbid supernatant was disintegrated with an ultrasonication instrument (APTIO-1200D, Nanjing Xianou Instruments Manufacture Co. Ltd., Nanjing, China) equipped with a 20 mm cylindrical titanium alloy probe to obtain nanocelluloses. First, the ultrasonication was conducted in an ice bath to keep the temperature below 40 °C with an output power of 600 W with 2/2 s on/off pulses for 10 min to individualize cellulose nanocrystals (OA-CNC). Then, the larger neutralized residual particles were diluted to 0.2 wt%, and were subjected to ultrasonication treatment for 30 min at 600 W in the same configuration as mentioned above to produce cellulose nanofibers (OA-CNF).

For the reference, the raw luffa and DES-treated luffa were acid hydrolyzed in 60% w/w sulfuric acid solution with a biomass to acid ratio of 1:30 at 50 °C for 60 min to provide cellulose nanocrystals and nanofibers for comparison. The washing/separation and ultrasonication procedures were similar to those used for the OA-CNC and OA-CNF. The obtained CNC and CNF from sole sulfuric acid hydrolysis were referred as SA-CNC and SA-CNF, respectively, and the samples collected from the combined DES treatment and sulfuric acid hydrolysis were named OS-CNC and OS-CNF, respectively. All samples were lyophilized for 48 h to calculate the mass yields.

Characterization of nanocelluloses

Nanocellulose suspension (0.01 wt%) was deposited onto glow-discharged carbon-coated TEM grids (300 mesh copper, formvar/carbon, Ted Pella Inc., Redding, CA, USA) and the excess liquid was removed by blotting with a filter paper after 10 min. The specimens were allowed to dry under ambient conditions. The samples were

observed using a JEM-1400 transmission electron microscope (JEOL Ltd., Japan) operated at 100 kV accelerating voltage.

For the FTIR spectra (VERTEX 80v spectrometer, Bruker, Germany) KBr pellets (1:100, w/w) were fabricated from freeze-dried nanocelluloses. The spectra were collected under ambient conditions in the transmittance mode from an accumulation of 128 scans at a 4 cm^{-1} resolution over the regions of 400–4000 cm^{-1}.

The surface charge of lignin containing nanocellulose was measured using a zeta potential (ZP) analyzer (Nanobrook Omni, Brookhaven Instruments, Holtsville, NY, USA) from an aqueous suspension (~0.5g/cm^{-3}).

XRD powder diffractometer (D8 Advance, Bruker, Germany) with Cu Kα radiation at an operating voltage of 40 kV, and a filament current of 40 mA was used to study the crystal structure of the lyophilized lignin containing nanocellulose. The samples were ground into powder and spread on the sample plate, followed by a slight press with a glass slide.

The thermal properties, including the determination of dehydration, degradation, and thermal transitions, were studied with a NETZSCH STA 449C thermal analyzer (Germany). The measurements were conducted in a nitrogen atmosphere from room temperature to 600 °C with a heating rate of 10 °C/min.

Preparation and characterization of lignin containing nanocellulose films

The 0.2 wt% cellulose nanofiber suspensions were vacuum-filtered on a polyvinylidene fluoride (PVDF) membrane (pore size 0.65 μm) to prepare wet sheets. Subsequently, the wet sheets were covered by another PVDF film and compressed between two paper sheets at 93 °C in a vacuum under pressure of 800 mbar for 10 min. The obtained films had a grammage of ~80 g/m^2.

The mechanical properties of nanocellulose films were analyzed by measuring the tensile stress and strain at break with a universal testing machine (Zwick/Roell D0724587, Switzerland) equipped with a 100 N load cell. The films were cut into

strips of 5 mm in width, and their thickness was measured using a precision thickness gauge (Hanatek FT3, Hanatek Instruments, UK). Before the test, the strips were conditioned in the measurement environment (relative humidity of 50% at 23 °C) for at least 24 h.

3. Results and discussion

Effect of reaction conditions of DES treatment on the chemical compositions of luffa

First, the luffa biomass was treated with a ChCl-OA DES at four different temperatures (70, 80, 90, and 100 °C) for 120 min. The luffa's mass yields and composition are shown in Figure 1. The mass yield decreased significantly as a function of temperature (Figure 1a), ranging from 76.8 to 48.0 wt%. The high acidity of oxalic acid (pK_{a1} = 1.25 and pK_{a2} = 4.14) degrades both the carbohydrates and the lignin in luffa, and high temperatures further facilitate the degradation reactions and decrease the solid yield (Zhang et al., 2016). The luffa's detailed composition is shown in Figure 1b, which illustrates the contents of cellulose, hemicellulose, and lignin in the liquid and solid fractions after the DES treatment. The dissolution and removal of all main biomass constituents were promoted by the increase of the temperature in the DES treatment. Especially hemicelluloses were noted to be the most susceptible to chemical and thermal degradation, which resulted in their extended removal (9.7–13.6 wt% in soluble fractions), presumably due to the acidic hydrolysis reactions (Alvarezvasco et al., 2016; Hendriks and Zeeman, 2009). Moreover, a high delignification degree, i.e., removal of lignin, was achieved at higher temperatures. For example, 24.4 wt% and 33.8 wt% of the lignin was extracted at 70 and 80 °C, respectively, while an increase of the temperature to 90 and 100 °C resulted in a removal rate of up to 59.3 wt% and 72.9 wt%, respectively. Previously, a lignin removal of 57.9 and 53.1 wt% had been achieved with a ChCl-OA DES using wheat straw and corncob biomasses (Jablonský et al., 2015; Zhang et al., 2016). At the same time, the hydrolysis reactions of cellulose were also promoted at high

temperatures, and its solubility ranged from 9.2 wt% at 70 °C, to 13.8 wt % at 80 °C, to 15.5 wt% at 90 °C, and to 26.4 wt% at 100 °C. The reaction temperature of 90 °C, which resulted in a relatively high cellulose content, was used for the subsequent experiments to investigate the role of the reaction time on the fractionation efficiency.

Similar to temperature, the prolongation of the reaction time of the DES treatment resulted in a decrease of the mass yield of the biomass, but the effect was smaller (Figure 1c). With the prolongation of the treatment time from 60 to 150 min (Figure 1d), the degree of delignification gradually increased from 32.0 to 64.1 wt%. However, a treatment time of 150 min led to the lowest dissolution loss of cellulose, as previously reported with a DES treatment of wood celluloses (Sirviö et al., 2016). The reason for this phenomenon is the formation of esters (monoester or cross-linked diester) between hydroxyl groups of cellulose with oxalic acid, which can prevent the dissolution and hydrolysis of cellulose. For the subsequent experiments, a temperature of 90 °C and a reaction time of 150 min were selected as optimal fractionation conditions for the fabrication of nanocelluloses from the cellulose-rich solid fraction.

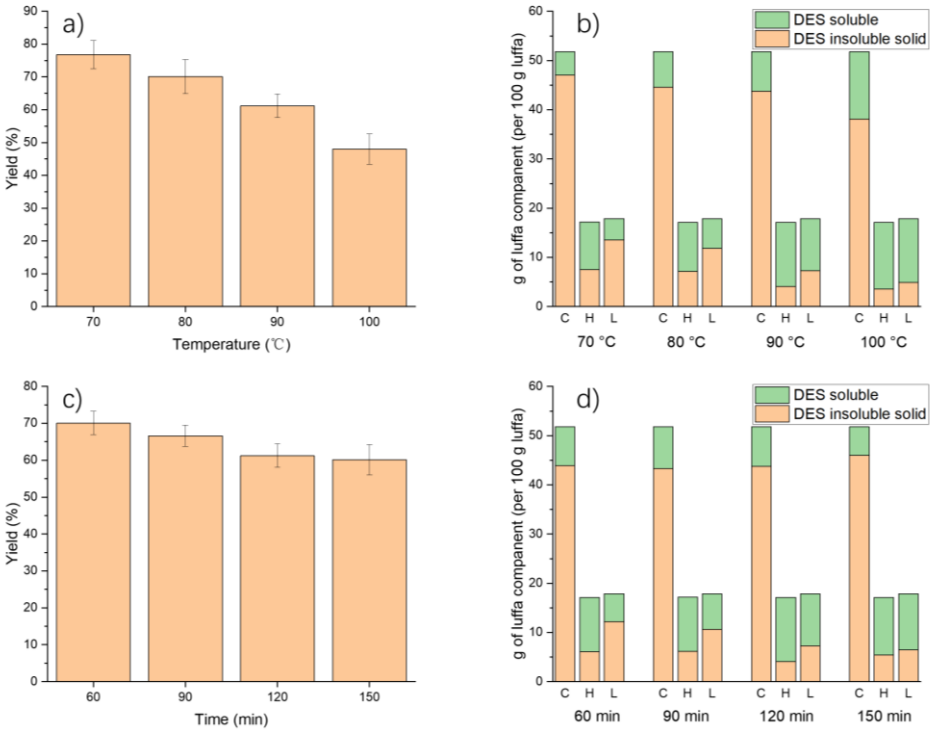

Figure 1. (a) Mass yield of luffa after DES treatment at different temperature, (b) composition of soluble and solid fractions after DES treatment at different temperature (C = cellulose, H = hemicellulose, L = lignin), (c) mass yield of luffa after DES treatment with different reaction time at 90°C, and (d) composition of soluble and solid fractions after DES treatment with different reaction time at 90°C.

Characterizations of the luffa before and after the DES treatment

Figure 2 presents the scanning electron microscopy (SEM) images of the raw luffa and the luffa after the DES treatment (at 90 °C for 150 min). It was observed that the fiber structure of the luffa was partially degraded during the acidic DES treatment (Figures 2a and 2c). The pristine luffa consisted of short fibrous particles with a typical length of a few millimeters, while powder like, roundish particles were observed after the DES treatment. The diameter of these particles was mostly less than 0.4 mm. When further magnified (x500), the surface of the treated luffa was seen to be rougher, and separated fibers could be observed. These changes are presumably attributed to the removal of hemicellulose and lignin during the ChCl-OA DES treatment. The XRD patterns of the pristine luffa and the luffa after the DES treatment are shown in Figure 2e. The XRD diffractograms of both the pristine and the DES-treated luffa exhibited the typical characteristics of the cellulose I structure. The crystallinity index (CrI) values calculated from the XRD patterns using the Segal method (Segal et al., 1959) were 67.6% for the untreated luffa and 80.3% for the DES-treated luffa. This increase in crystallinity is likely due to the removal of hemicellulose and lignin during the DES treatment (Zhang et al., 2016). In addition, the hydrolysis and dissolution of amorphous cellulose may have contributed to the crystallinity values (Liu et al., 2017a).

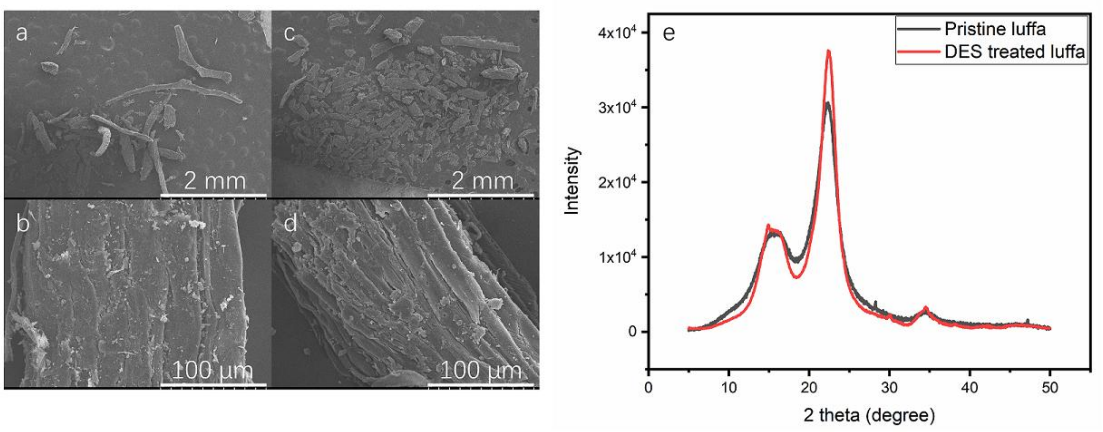

Figure 2. Scanning electron microscopy (SEM) images of (a) pristine luffa, x25 SE, (b) initial luffa, x500 SE, (c) DES-treated luffa (at temperature of 90 °C for 150 min), x25 SE, (d) DES-treated luffa, x500 SE, and (e) XRD patterns of pristine and DES-treated luffa.

The yield and morphology of nanocelluloses

After the DES treatment, the residue was washed and separated by centrifugation, i.e. turbid supernatant and solid residue. The followed ultrasonication treatment for these two parts led to CNC (turbid supernatant) and CNF (solid residue), respectively. Through the TEM results (see below, Figure 4), the residual parts are all long fiber-like (> 500 nm in length). CNCs are rod-like or whisker-shaped nanoparticles with 3-5 nm in width and 50-500 nm in length. As CNFs are typically produced through mechanical refining, the nanoparticles have a higher aspect ratio with 4-20 nm in width and 500-2000 nm in length (Moon et al., 2011). Therefore, we defined the residual parts as CNF. The DES-treated (at 90 °C for 150 min) luffa was disintegrated into nanocelluloses with an ultrasonication process, which resulted in lignin containing cellulose nanofiber (OA-CNF) and nanocrystal (OA-CNC) fractions. The reference samples were fabricated with a sulfuric acid treatment for both the DES-treated luffa and the pristine luffa (OS-nanocelluloses and SA-nanocelluloses, respectively). The total nanocellulose amount and the mass yields of the CNF and CNC fractions of the three production approaches are shown in Figure 3. The acidic DES treatment resulted in the highest total nanocellulose yield but had the lowest proportion of CNC fractions. Presumably, the DES complex of ChCl and OA failed to

impregnate and dissolve the cellulose structure efficiently because of the high surface lignin content (Bian et al., 2017a). Sulfuric acid was more prone to hydrolyzing the cellulose chains and resulted in higher CNC yields. However, it also caused significant yield losses. In addition, the more severe hydrolysis caused by the sulfuric acid was seen as lower viscosity of the nanocellulose suspensions. The OA-CNF manifested as highly viscous gel-like suspensions, while the OS-CNF and SA-CNF were more liquid-like low-viscosity solutions. In previous studies, the mass ratio of cellulose raw materials to ChCl-OA DES was between 1:45 and 1:100, with a treatment time of 2–6 h and temperatures of 80–120 °C (Ling et al., 2019; Sirviö et al., 2016; Yang et al., 2019). In this study, the mass ratio of luffa to DES was 1:20, which is much higher than previously reported. In addition, the treatment time was relatively short. These milder and optimized reaction conditions improve both the material and the energy efficiency of the DES treatment.

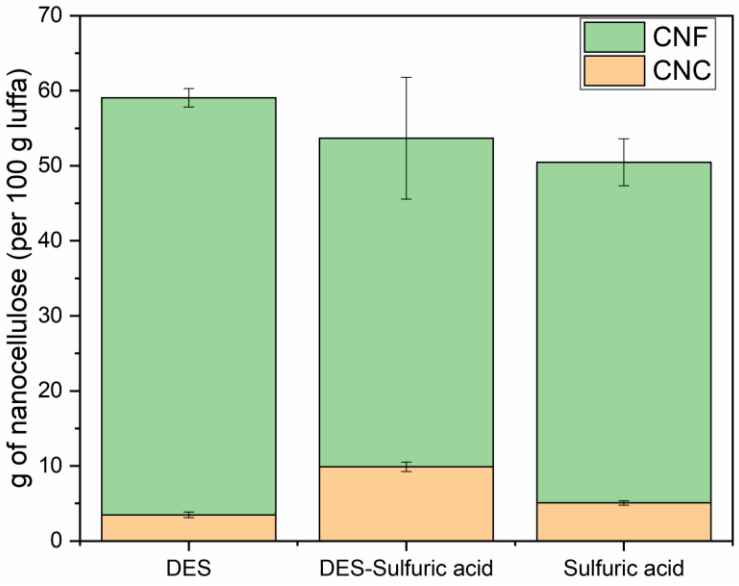

Figure 3. Total nanocellulose amount and yields of cellulose nanofibers (CNF) and nanocrystals (CNC) from DES treatment (at 90 °C for 150 min), combined DES and sulfuric acid treatments, and sulfuric acid hydrolysis.

The micromorphology of the CNC and CNF fractions was analyzed using TEM. As shown in Figure 4, a clear difference can be seen between the shapes and sizes of the OA-CNC (Figure 4a), OS-CNC (Figure 4b), and SA-CNC (Figure 4c). Both the

sulfuric acid-treated samples (OS-CNC and SA-CNC) contained particles with smaller particle sizes and aspect ratios than the OA-CNC. The diameter ranged from 15 to 40 nm for SA-CNC and from 14 to 49 nm for OS-CNC, while the length was 190–560 nm and 215–820 nm, respectively. These samples also contained dark, roundish particles, which may have originated from lignin (Figures 4b and 4c, pointed by arrows) (Li et al., 2019). The OA-CNC consisted of a mixture of short needlelike crystals and elongated nanofibers with diameters ranging from 11 to 28 nm and lengths between 188 and 3125 nm, indicating only partial hydrolysis of cellulose. This result may be due to milder reaction conditions and the existence of lignin, which hinders the hydrolysis reaction; previously, rod-like CNC were obtained with a yield of 66–88% using the same DES with cotton or cellulose pulp from softwood (Liu et al., 2017a; Sirviö et al., 2016). To conclude, the morphology of produced nanocellulose will be mainly impacted by the presence of lignin.

The cellulose nanofibers from the DES-treated luffa (OA-CNF) (Figure 4d) had diameters ranging between 11 and 134 nm, their average diameter being 28 nm. The sample also contained larger residual fragments of luffa. The combined DES and acid hydrolysis treatments (OS-CNF) (Figure 4e) resulted in a more homogeneous and smaller size distribution with diameters ranging between 11 and 28 nm and with an average diameter of 19 nm. Interestingly, the direct sulfuric acid hydrolysis of the pristine luffa also produced well-dispersed SA-CNF suspensions (Figure 4f). The SA-CNF had diameters ranging from 10 to 42 nm, with an average diameter of 21 nm. Due to the low yield of CNC, the subsequent analysis was focused on the physicochemical properties of CNF fractions only.

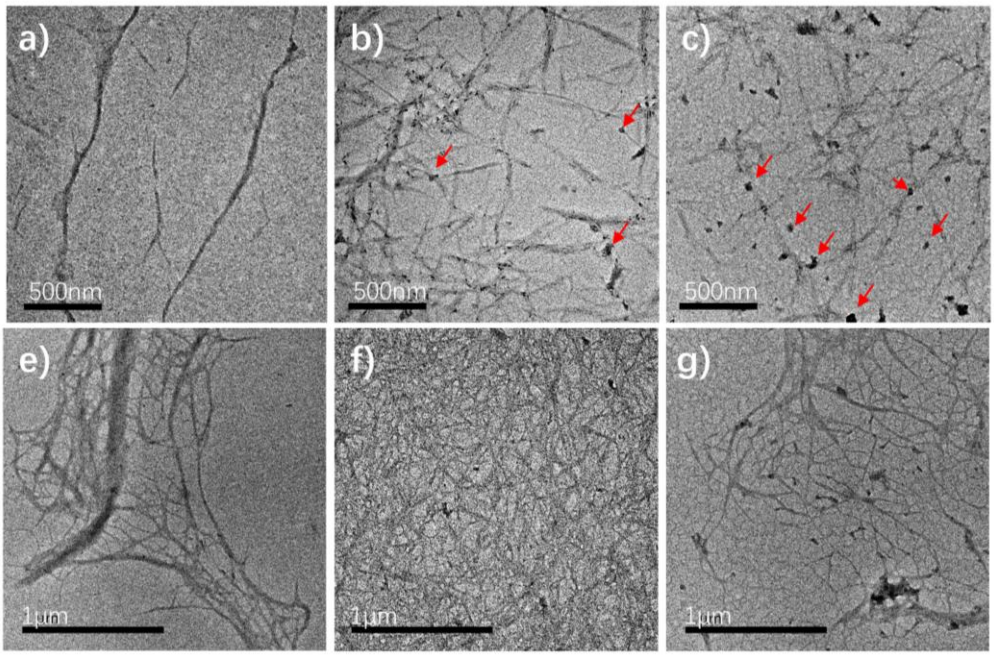

Figure 4. Transmission electron microscopy (TEM) images of cellulose nanocrystals and nanofibers from DES treatment (a and e, respectively), combined DES treatment and sulfuric acid hydrolysis (b and f, respectively), and sulfuric acid hydrolysis (c and g, respectively). The red arrows point to the lignin particles.

3.3 FTIR and XRD of nanocelluloses

The chemical structures of the pristine luffa and the cellulose nanofibers from the DES treatment, the combined DES and sulfuric treatment, and the sulfuric acid hydrolysis were analyzed using FTIR (Figure 5a). Absorption peaks appeared at 1429 cm^{-1}, 1161 cm^{-1}, and 896 cm^{-1} with the pristine luffa, which belong to the typical vibrations in cellulose (Schwanninger et al., 2004). The C=C stretching vibration of the aromatic ring in lignin was found at 1507 cm^{-1} and 1596 cm^{-1} (Schwanninger et al., 2004). After the DES treatment, the characteristic peaks of lignin almost disappeared, probably due to the decrease of the lignin content. Small peaks related to lignin were observed in OS-CNF and SA-CNF. This indicated that the lignin content in these two samples increased after the sulfuric acid hydrolysis. Especially in SA-CNF, the intensity of characteristic peaks of cellulose were much lower than the other two CNF. An absorption at 1740 cm^{-1} in the luffa was attributed to the acetyl and uronic ester groups of hemicelluloses (Alriols et al., 2009). This peak was very weak in OA-CNF,

OS-CNF, and SA-CNF (almost disappeared) because of the removal of the hemicelluloses. The carbonyl vibrations of the ester and carboxylic acid groups (1740 cm^{-1} (Sirviö et al., 2016) were absent from OA-CNF and OS-CNF, which could be due to the existence of lignin on nanofiber surfaces, mitigating the esterification of the cellulose in a way similar to that previously reported (Bian et al., 2017a). The low zeta potential value of OA-CNF (-12.4 mV) supported this finding.

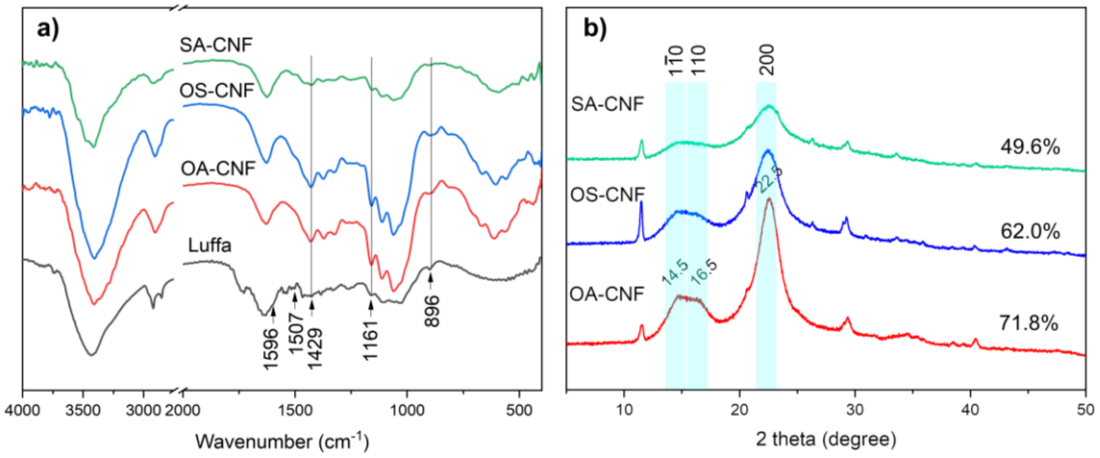

Figure 5. FTIR spectra of (a) pristine luffa and cellulose nanofibers from DES treatment (OA-CNF), combined DES and sulfuric acid treatments (OS-CNF) and sulfuric acid hydrolysis (SA-CNF), and (b) XRD diffraction patterns of cellulose nanofibers.

The crystalline structure of freeze-dried CNF samples was analyzed using X-ray diffraction (Figure 5b). Similar to the original luffa (Figure 2e), typical diffraction peaks associated to cellulose I were also detected in all CNF. These peaks were located at 2 theta around 14.5°, 16.5°, and 22.5°, and were attributed to the crystalline planes of ($1\bar{1}0$), (110), and (200), respectively. The sharp and intense peaks around 11.6°, 29.5°, and 41° may have been caused by impurities, which were also observed in previous studies (de Morais Teixeira et al., 2010; Ewulonu et al., 2019; Liu et al., 2016). However, the CrI values of the CNF showed significant differences. The sulfuric acid treatment decreased the CrI remarkably since the highest value of 71.8% was obtained with OA-CNF, while the OS-CNF and SA-CNF had CrI values of 62.0% and 49.6%, respectively. These results correlated with the lignin contents of the samples, which were 10.7 wt% for OA-CNF, 12.7 wt% for OS-CNF, and 22.6 wt%

for SA-CNF. On the other hand, the strong acid usually resulted in the hydrolysis of the amorphous region and a higher crystallinity, but it could also damage the crystalline region and lead to low crystallinity (Liu et al., 2016).

3.5 Thermal stability

The thermogravimetric analysis (TGA) and the differential thermal analysis (DTA) of the cellulose nanofiber samples are presented in Figure 6. The most significant mass loss with all samples was noted between 200 and 400 °C, which is related to the thermal decomposition of the main biomass constituents, while the minor mass loss below 200 °C was because of moisture evaporation. Above 400 °C, the samples were charred. The degradation temperature and maximum mass loss are shown in Figure 6b. It was noted that SA-CNF had two T_{max} temperatures, which were T_{max1} at 286.9 °C and T_{max2} at 348.1 °C and were likely due to the high lignin content of the sample (Hong et al., 2016). It has previously been reported that when the lignin content in cellulose drops below 18.6 wt%, only one T_{max} temperature is observed (Wen et al., 2019). Consequently, both the OA-CNF and the OS-CNF, which had a lower lignin content (10.7 wt% and 12.7 wt%, respectively), possessed only the sole T_{max} temperature at 342.8 °C. This value was slightly lower than that of SA-CNF (T_{max2} = 348.1 °C). It is possible that the high thermal stability of lignin can protect the SA-CNF from decomposition and increase its thermal stability. However, the T_{max} of both the OA-CNF and the OS-CNF was higher than that typically obtained with pure nanocellulose with a high cellulose content. For example, T_{max} has been reported to range from 219 to 308 °C for cotton fiber and microcrystalline cellulose from cotton (Liu et al., 2017a).

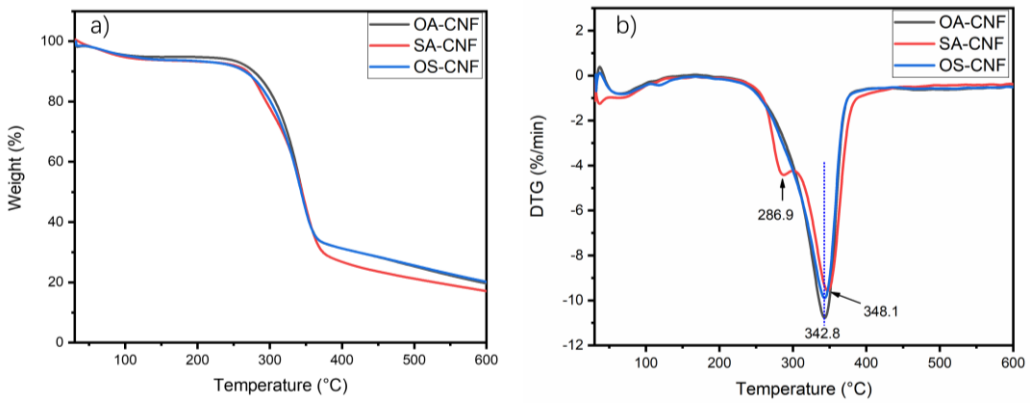

Figure 6. (a) Thermogravimetric analysis (TGA) and (b) DTG curves of cellulose nanofibers from DES treatment (OA-CNF), combined DES and sulfuric acid treatments (OS-CNF), and sulfuric acid hydrolysis (SA-CNF).

3.5 Mechanical properties of nanocellulose films

Self-standing films were prepared from cellulose nanofiber samples using a filtration method. The typical tensile stress-strain curves of the films are shown in Figure 7, and their mechanical characteristics are given in Table 1. In general, the OA-CNF film exhibited the highest tensile strength (134 MPa), which is very close to the strength previously reported for some pure cellulose nanofibers films, e.g., 132 MPa (Farooq et al., 2019) and 138 MPa (Cherpinski et al., 2018). Moreover, the tensile strength of OA-CNF films was similar to or higher than most recently reported lignin containing nanocellulose films, e.g., 132 MPa with 4% lignin (Rojo et al., 2015), 97 MPa with 14% lignin (Rojo et al., 2015), 99.3 MPa with 12–13% lignin (Cherpinski et al., 2018), and 64.7 MPa with 28.6% lignin (Li et al., 2019). Both OS-CNF and SA-CNF had a lower tensile strength of 105 MPa and 114 MPa, respectively, which might be associated with their higher lignin content and lower aspect ratio of the samples. These factors can also cause a greater elongation of OA-CNF films (Chen et al., 2014; Cherpinski et al., 2018; Rojo et al., 2015; Smyth et al., 2017). It was also found that all the films were flexible (Figure 7a), but after folding (Figure 7b) and unfolding (Figure 7c), the OS-CNF and SA-CNF films split along the crease, while the OA-film maintained its structure. Lignin acts as a cementitious component that increases stiffness, consistent with its stiffening role in

412 the native biomass cell wall (Rojo et al., 2015), which cause the rigidness of OS-CNF
413 and SA-CNF films. The lignin on nanocellulose can offer several advantages for its
414 derived films, such as UV blocking (Sirvio and Visanko, 2019), flame retardancy (Li
415 et al., 2019), and improved barrier properties (Rojo et al., 2015). Therefore, OA-CNF
416 can potentially be used to provide advanced characteristics for films and nanopapers.

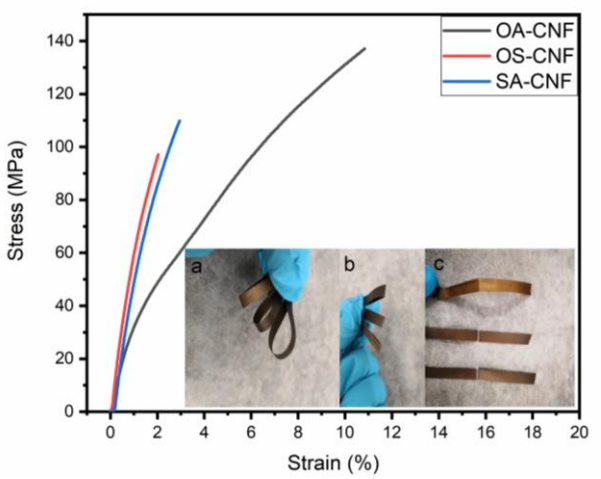

417

418 **Figure 7.** Typical tensile stress-strain curves of cellulose nanofiber films and visual appearance of
419 the films obtained from cellulose nanofibers from top to down, DES treatment (OA-CNF),
420 combined DES and sulfuric acid treatments (OS-CNF), and sulfuric acid hydrolysis (SA-CNF).

421 **Table 1** Mechanical properties of cellulose nanofiber films.

Sample	Elastic modulus (GPa)	Maximum tensile strength (MPa)	Elongation at break (%)	Thickness (μm)
OA-CNF	3.7±0.7	134±5	10.6±0.3	61.2±0.6
OS-CNF	8.0±0.3	105±12	2.2±0.3	46.0±1.1
SA-CNF	5.1±0.9	114±6	3.9±1.3	51.1±0.7

422 # 4. Conclusions

423 Acidic deep eutectic solvent treatment based on ChCl and oxalic acid dihydrate
424 was used to partially delignify non-wood luffa biomass and to facilitate the fabrication
425 of nanocelluloses. Under the optimal reaction condition of 90 °C for 150 min, a solid
426 fraction with cellulose content of 76.4 wt% and a residual lignin amount of 10.7 wt%
427 was produced. A two-step ultrasonication process of DES-treated luffa resulted in
428 lignin containing CNF (OA-CNF) and CNC (OA-CNC) fractions with a high total

yield of 59.1 wt%. The self-standing films produced from OA-CNF were flexible and foldable and exhibited a high tensile strength of 134 MPa and an elongation at break of 10.6%. This green approach based on acidic DESs provides a promising and sustainable method to individualize lignin containing nanocelluloses. This strategy has several potential advantages, such as high efficiency, low energy consumption, and use of environmentally friendly chemicals. Even could be further studied for tuning lignin content in biomass by control the reaction condition to obtain different lignin containing nanocellulose.

Acknowledgements

This research was supported by grants from the National Natural Science Foundation of China (31370567), the Doctorate Fellowship Foundation of Nanjing Forestry University, the National First-Class disciplines, the Priority Academic Program Development of Jiangsu Higher Education Institutions, and the Academy of Finland project “Bionanochemicals” (298295).

References:

Alriols, M.G., Tejado, A., Blanco, M.a., Mondragon, I., Labidi, J., 2009. Agricultural palm oil tree residues as raw material for cellulose, lignin and hemicelluloses production by ethylene glycol pulping process. Chem. Eng. J. 148, 106-114.

Alshaaer, M., Kailani, M.H., Ababneh, N., Mallouh, S.A.A., Sweileh, B., Awidi, A., 2017. Fabrication of porous bioceramics for bone tissue applications using luffa cylindrical fibres (LCF) as template. Process Appl. Ceram. 11, 13-20.

Alvarezvasco, C., Ma, R., Quintero, M., Guo, M., Geleynse, S., Ramasamy, K.K., Wolcott, M., Zhang, X., 2016. Unique low-molecular-weight lignin with high purity extracted from wood by deep eutectic solvents (DES): a source of lignin for valorization. Green Chem. 18, 5133-5141.

Bian, H.Y., Chen, L.H., Dai, H.Q., Zhu, J.Y., 2017a. Integrated production of lignin containing cellulose nanocrystals (LCNC) and nanofibrils (LCNF) using an easily recyclable di-carboxylic acid. Carbohydr. Polym. 167, 167-176.

Bian, H.Y., Chen, L.H., Gleisner, R., Dai, H.Q., Zhu, J.Y., 2017b. Producing wood-based nanomaterials by rapid fractionation of wood at 80 °C using a recyclable acid hydrotrope. Green Chem. 19, 3370-3379.

Bian, H.Y., Gao, Y., Luo, J., Jiao, L., Wu, W.B., Fang, G., Dai, H.Q., 2019. Lignocellulosic nanofibrils produced using wheat straw and their pulping solid residue: From agricultural waste to cellulose nanomaterials. Waste Manage. 91, 1-8.

Bian, H.Y., Gao, Y., Yang, Y.Q., Fang, G.G., Dai, H.Q., 2018. Improving cellulose nanofibrillation of waste wheat straw using the combined methods of prewashing, p-toluenesulfonic acid hydrolysis, disk grinding, and endoglucanase post-treatment. Bioresour. Technol. 256, 321-327.

Chen, L.H., Wang, Q.Q., Hirth, K., Baez, C., Agarwal, U.P., Zhu, J.Y., 2015. Tailoring the yield and characteristics of wood cellulose nanocrystals (CNC) using concentrated acid hydrolysis. Cellulose 22, 1753-1762.

Chen, W.S., Li, Q., Wang, Y.C., Yi, X., Zeng, J., Yu, H.P., Liu, Y.X., Li, J., 2014. Comparative Study of Aerogels Obtained from Differently Prepared Nanocellulose Fibers. Chemsuschem 7, 154-161.

Chen, Y., Su, N., Zhang, K., Zhu, S., Zhu, Z., Qin, W., Yang, Y., Shi, Y., Fan, S., Wang, Z., 2018. Effect of fiber surface treatment on structure, moisture absorption and mechanical properties of luffa sponge fiber bundles. Ind. Crops Prod. 123, 341-352.

Cherpinski, A., Torres-Giner, S., Vartiainen, J., Peresin, M.S., Lahtinen, P., Lagaron, J.M., 2018. Improving the water resistance of nanocellulose-based films with polyhydroxyalkanoates processed by the electrospinning coating technique. Cellulose 25, 1291-1307.

de Morais Teixeira, E., Corrêa, A.C., Manzoli, A., de Lima Leite, F., de Oliveira, C.R., Mattoso, L.H.C., 2010. Cellulose nanofibers from white and naturally colored cotton fibers. Cellulose 17, 595-606.

Demir, H., Atikler, U., Balköse, D., Tıhmınlıoğlu, F., 2006. The effect of fiber surface treatments on the tensile and water sorption properties of polypropylene–luffa fiber composites. Composites Part A 37, 447-456.

Diop, C.I.K., Tajvidi, M., Bilodeau, M.A., Bousfield, D.W., Hunt, J.F., 2017. Evaluation of the incorporation of lignocellulose nanofibrils as sustainable adhesive replacement in medium density fiberboards. Ind. Crops Prod. 109, 27-36.

Dou, J., Bian, H., Yelle, D.J., Ago, M., Vajanto, K., Vuorinen, T., Zhu, J., 2019. Lignin containing cellulose nanofibril production from willow bark at 80 degrees using a highly recyclable acid hydrotrope. Ind. Crops Prod. 129, 15-23.

Ewulonu, C.M., Liu, X., Wu, M., Huang, Y., 2019. Ultrasound-assisted mild sulphuric acid ball milling preparation of lignocellulose nanofibers (LCNFs) from sunflower stalks (SFS). Cellulose 26, 4371-4389.

Fan, Y., Saito, T., Isogai, A., 2008. Chitin nanocrystals prepared by TEMPO-mediated oxidation of alpha-chitin. Biomacromolecules 9, 192-198.

Farooq, M., Zou, T., Riviere, G., Sipponen, M.H., Osterberg, M., 2019. Strong, Ductile, and Waterproof Cellulose Nanofibril Composite Films with Colloidal Lignin Particles. Biomacromolecules 20, 693-704.

Guo, Z., Zhang, Q., You, T., Zhang, X., Xu, F., Wu, Y., 2019. Short-time deep eutectic solvent pretreatment for enhanced enzymatic saccharification and lignin valorization. Green Chem. 21, 3099-3108.

Hendriks, A., Zeeman, G., 2009. Pretreatments to enhance the digestibility of lignocellulosic biomass. Bioresour. Technol. 100, 10-18.

Hoeger, I.C., Nair, S.S., Ragauskas, A.J., Deng, Y.L., Rojas, O.J., Zhu, J.Y., 2013. Mechanical deconstruction of lignocellulose cell walls and their enzymatic saccharification. Cellulose 20, 807-818.

Hong, S., Lian, H.L., Sun, X., Pan, D., Carranza, A., Pojman, J.A., Motamorales, J.D., 2016. Zinc-based deep eutectic solvent-mediated hydroxylation and demethoxylation of lignin for the production of wood adhesive. RSC Adv. 6, 89599-89608.

Huang, Y., Sudhakaran Nair, S., Chen, H., Fei, B., Yan, N., Feng, Q., 2019. Lignin rich nanocellulose fibrils isolated from parenchyma cells and fiber cells of western red cedar bark. ACS Sustainable Chem. Eng. 7, 15607-15616.

Jablonský, M., Škulcová, A., Kamenská, L., Vrška, M., Šima, J., 2015. Deep eutectic solvents: fractionation of wheat straw. Bioresources 10, 8039-8047.

Jablonsky, M., Skulcova, A., Malvis, A., Sima, J., 2018. Extraction of value- added components from food industry based and agro-forest biowastes by deep eutectic solvents. J. Biotechnol. 282, 46-66.

Lacerda, T.M., Zambon, M.D., Frollini, E., 2015. Oxalic acid as a catalyst for the hydrolysis of sisal pulp. Ind. Crops Prod. 71, 163-172.

Laidani, Y., Hanini, S., Henini, G., 2011. Use of fiber Luffa cylindrica for waters traitement charged in copper. Study of the possibility of its regeneration by desorption chemical. Energy Procedia 6, 381-388.

Lee, M., Heo, M.H., Lee, H., Lee, H.-H., Jeong, H., Kim, Y.-W., Shin, J., 2018. Facile and eco-friendly extraction of cellulose nanocrystals via electron beam irradiation followed by high-pressure homogenization. Green Chem. 20, 2596-2610.

Li, P., Sirviö, J.A., Hong, S., Ämmälä, A., Liimatainen, H., 2019. Preparation of Flame-retardant Lignin-containing Wood Nanofibers Using a High-consistency Mechano-chemical Pretreatment. Chem. Eng. J. 375, 122050.

Ling, Z., Edwards, J.V., Guo, Z., Prevost, N.T., Nam, S., Wu, Q., French, A.D., Xu, F., 2019. Structural variations of cotton cellulose nanocrystals from deep eutectic solvent treatment: micro and nano scale. Cellulose 26, 861-876.

Liu, C., Li, B., Du, H., Lv, D., Zhang, Y., Yu, G., Mu, X., Peng, H., 2016. Properties of nanocellulose isolated from corncob residue using sulfuric acid, formic acid, oxidative and mechanical methods. Carbohydr. Polym. 151, 716-724.

Liu, Y., Guo, B., Xia, Q., Meng, J., Chen, W., Liu, S., Wang, Q., Liu, Y., Li, J., Yu, H., 2017a. Efficient cleavage of strong hydrogen bonds in cotton by deep eutectic solvents and facile fabrication of cellulose nanocrystals in high yields. ACS Sustainable Chem. Eng. 5, 7623-7631.

Liu, Y.Z., Chen, W.S., Xia, Q.Q., Guo, B.T., Wang, Q.W., Liu, S.X., Liu, Y.X., Li, J., Yu, H.P., 2017b. Efficient Cleavage of Lignin-Carbohydrate Complexes and Ultrafast Extraction of Lignin Oligomers from Wood Biomass by Microwave-Assisted Treatment with Deep Eutectic Solvent. Chemsuschem 10, 1692-1700.

Lynam, J.G., Kumar, N., Wong, M.J., 2017. Deep eutectic solvents' ability to solubilize lignin, cellulose, and hemicellulose; thermal stability; and density. Bioresour. Technol. 238, 684-689.

Ma, Y., Xia, Q., Liu, Y., Chen, W., Liu, S., Wang, Q., Liu, Y., Li, J., Yu, H., 2019. Production of Nanocellulose Using Hydrated Deep Eutectic Solvent Combined with Ultrasonic Treatment. ACS Omega 4, 8539-8547.

Mao, J., Abushammala, H., Hettegger, H., Rosenau, T., Laborie, M.-P., 2017. Imidazole, a new tunable reagent for producing nanocellulose, part I: Xylan-coated CNCs and CNFs. Polymers 9, 473.

Meng, X., Parikh, A., Seemala, B., Kumar, R., Pu, Y., Wyman, C.E., Cai, C.M., Ragauskas, A.J., 2019. Characterization of fractional cuts of co-solvent enhanced lignocellulosic fractionation lignin isolated by sequential precipitation. Bioresour. Technol. 272, 202-208.

Moon, R.J., Martini, A., Nairn, J., Simonsen, J., Youngblood, J., 2011. Cellulose nanomaterials review: structure, properties and nanocomposites. Chem. Soc. Rev. 40, 3941-3994.

Nair, S.S., Chen, H.Y., Peng, Y., Huang, Y.H., Yan, N., 2018. Polylactic Acid Biocomposites Reinforced with Nanocellulose Fibrils with High Lignin Content for Improved Mechanical, Thermal, and Barrier Properties. ACS Sustainable Chem. Eng. 6, 10058-10068.

Nair, S.S., Kuo, P.-Y., Chen, H., Yan, N., 2017. Investigating the effect of lignin on the mechanical, thermal, and barrier properties of cellulose nanofibril reinforced epoxy composite. Ind. Crops Prod. 100, 208-217.

Nair, S.S., Yan, N., 2015. Effect of high residual lignin on the thermal stability of nanofibrils and its enhanced mechanical performance in aqueous environments. Cellulose 22, 3137-3150.

Nascimento, S.A., Rezende, C.A., 2018. Combined approaches to obtain cellulose nanocrystals, nanofibrils and fermentable sugars from elephant grass. Carbohydr. Polym. 180, 38-45.

Osong, S.H., Norgren, S., Engstrand, P., 2013. An approach to produce nano-ligno-cellulose from mechanical pulp fine materials. Nord Pulp Pap Res J 28, 472-479.

Poletto, M., Zattera, A.J., Santana, R.M.C., 2012. Thermal decomposition of wood: Kinetics and degradation mechanisms. Bioresour. Technol. 126, 7-12.

Rojo, E., Peresin, M.S., Sampson, W.W., Hoeger, I.C., Vartiainen, J., Laine, J., Rojas, O.J., 2015. Comprehensive elucidation of the effect of residual lignin on the physical, barrier, mechanical and surface properties of nanocellulose films. Green Chem. 17, 1853-1866.

Rosa, M.F., Medeiros, E.S., Malmonge, J.A., Gregorski, K.S., Wood, D.F., Mattoso, L.H.C., Glenn, G., Orts, W.J., Imam, S.H., 2010. Cellulose nanowhiskers from coconut husk fibers: Effect of preparation conditions on their thermal and morphological behavior. Carbohydr. Polym. 81, 83-92.

Sadeghifar, H., Venditti, R., Jur, J., Gorga, R.E., Pawlak, J.J., 2017. Cellulose-Lignin Biodegradable and Flexible UV Protection Film. ACS Sustainable Chem. Eng. 5, 625-631.

Saito, T., Isogai, A., 2004. TEMPO-mediated oxidation of native cellulose. The effect of oxidation conditions on chemical and crystal structures of the water-insoluble fractions. Biomacromolecules 5, 1983-1989.

Schwanninger, M., Rodrigues, J., Pereira, H., Hinterstoisser, B., 2004. Effects of short-time vibratory ball milling on the shape of FT-IR spectra of wood and cellulose. Vib. Spectrosc 36, 23-40.

Segal, L., Creely, J., Martin Jr, A., Conrad, C., 1959. An empirical method for estimating the degree of crystallinity of native cellulose using the X-ray diffractometer. Text. Res. J. 29, 786-794.

Shen, J., Xie, Y.M., Huang, X., Zhou, S., Ruan, D., 2012. Mechanical properties of luffa sponge. J. Mech. Behav. Biomed. Mater. 15, 141-152.

Shen, X.J., Wen, J.L., Mei, Q.Q., Chen, X., Sun, D., Yuan, T.Q., Sun, R.C., 2019. Facile fractionation of lignocelluloses by biomass-derived deep eutectic solvent (DES) pretreatment for cellulose enzymatic hydrolysis and lignin valorization. Green Chem. 21, 275-283.

Siqueira, G., Bras, J., Dufresne, A., 2010. Luffa Cylindrica as a Lignocellulosic Source Of Fiber, Microfibrillated Cellulose, And Cellulose Nanocrystals. Bioresources 5, 727-740.

Sirviö, J.A., Visanko, M., Liimatainen, H., 2016. Acidic deep eutectic solvents as hydrolytic media for cellulose nanocrystal production. Biomacromolecules 17, 3025-3032.

Sirvio, J.A., Visanko, M., 2019. Highly Transparent Nanocomposites Based on Poly(vinyl alcohol) and Sulfated UV-Absorbing Wood Nanofibers. Biomacromolecules 20, 2413-2420.

Sluiter, A., Hames, B., Ruiz, R., Scarlata, C., Sluiter, J., Templeton, D., Crocker, D., 2010. Determination of structural carbohydrates and lignin in biomass. Laboratory analytical procedure.

Smyth, M., García, A., Rader, C., Foster, E.J., Bras, J., 2017. Extraction and process analysis of high aspect ratio cellulose nanocrystals from corn (Zea mays) agricultural residue. Ind. Crops Prod. 108, 257-266.

Spence, K.L., Venditti, R.A., Rojas, O.J., Habibi, Y., Pawlak, J.J., 2010. The effect of chemical composition on microfibrillar cellulose films from wood pulps: water interactions and physical properties for packaging applications. Cellulose 17, 835-848.

Wen, Y.B., Yuan, Z.Y., Liu, X.L., Qu, J.L., Yang, S., Wang, A., Wang, C.P., Wei, B., Xu, J.F., Ni, Y.H., 2019. Preparation and Characterization of Lignin-Containing Cellulose Nanofibril from Poplar High-Yield Pulp via TEMPO-Mediated Oxidation and Homogenization. ACS Sustainable Chem. Eng. 7, 6131-6139.

Yang, X., Xie, H., Du, H., Zhang, X., Zou, Z., Zou, Y., Liu, W., Lan, H., Zhang, X., Si, C., 2019. Facile Extraction of Thermally Stable and Dispersible Cellulose Nanocrystals with High Yield via a Green and Recyclable FeCl3-Catalyzed Deep Eutectic Solvent System. ACS Sustainable Chem. Eng. 7, 7200-7208.

Zampieri, A., Mabande, G.T., Selvam, T., Schwieger, W., Rudolph, A., Hermann, R., Sieber, H., Greil, P., 2006. Biotemplating of Luffa cylindrica sponges to self-supporting hierarchical zeolite macrostructures for bio-inspired structured catalytic reactors. Mat. Sci. Eng. C-Bio. S. 26, 130-135.

Zhang, C.-W., Xia, S.-Q., Ma, P.-S., 2016. Facile pretreatment of lignocellulosic biomass using deep eutectic solvents. Bioresour. Technol. 219, 1-5.

*Declaration of Interest Statement

Conflict of interest

I hereby declare that:
We have no financial and personal relationships with other people or organizations that can inappropriately influence our work, there is no professional or other personal interest of any nature or kind in any product, service and/or company that could be construed as influencing the position presented in the manuscript of "Production and characterization of lignin containing nanocellulose from luffa through an acidic deep eutectic solvent treatment and systematic fractionation**".** No potential conflict of interest was reported by the authors.

Hailan Lian, Ph.D

Nanjing Forestry University, Nanjing, China.